Vol. **108** (2005) *ACTA PHYSICA POLONICA A* No. 5

Proceedings of the XXXIV International School of Semiconducting Compounds, Jaszowiec 2005

Fano Resonance of Eu^{2+} and Eu^{3+} in (Eu,Gd)Te MBE Layers

B.A. Orlowski[a], B.J. Kowalski[a], P. Dziawa[a], M. Pietrzyk[a], S. Mickievicius[b], V. Osinniy[a], B. Taliashvili[a], I.A. Kowalik[a], T. Story[a] and R.L. Johnson[c]

[a]Institute of Physics, Polish Academy of Sciences
al. Lotników 32/46, 02-668 Warsaw, Poland
[b]Semiconductor Physics Institute, A. Gostauto 11, 2600 Vilnius, Lithuania
[c]Institut für Experimentalphysik, Universität Hamburg
Luruper Chaussee 149, 22761 Hamburg, Germany

Resonant photoemission spectroscopy, with application of synchrotron radiation, was used to study the valence band electronic structure of clean surface of (EuGd)Te layers. Fano-type resonant photoemission spectra corresponding to the Eu $4d-4f$ transition were measured to determine the contribution of $4f$ electrons of Eu^{2+} and Eu^{3+} ions to the valence band. The resonant and antiresonant photon energies of Eu^{2+} ions were found as equal to 141 eV and 132 eV, respectively and for Eu^{3+} ions were found as equal to 146 eV and 132 eV, respectively. Contribution of $Eu^{2+}4f$ electrons was found at the valence band edge while for Eu^{3+} it was located in the region between 3.5 eV and 8.5 eV below the valence band edge.

PACS numbers: 79.60.–i, 71.20.Mq

1. Introduction

The rare earth chalcogenides, like EuTe, belong to the family of ionic Heisenberg magnetic semiconductors [1]. In EuTe doped with Gd, Gd^{3+} ions substitute Eu^{2+} ions. As a result, the Gd $5d$ electrons become conducting electrons in such a system. So, EuTe crystal doped by this method becomes a conducting material. The appearance of conducting electrons leads to the qualitative changes in magnetic properties of $Eu_{1-x}Gd_xTe$ solid solution. In this case, due to the RKKY interaction, under particular conditions, the antiferromagnetic order observed in insulating layers of EuTe can be replaced by ferromagnetic state in n-type

$Eu_{1-x}Gd_xTe$ layer. This new property can make the material suitable for future spintronic applications, e.g. in spin filters [2, 3].

2. Resonant photoemission

During the last 20 years, resonant photoemission spectroscopy (RPS) [4–6] has been developed into a powerful tool for investigations of solids [7, 8]. This method allows us to distinguish the contribution of rare earth $4f$ electrons to the valence band density of states. In particular, it permits to distinguish the contribution of Eu $4f$ electrons to the valence band of (EuGd)Te crystal. It is based on a Fano effect [9] and it leads to an increase in photoemission intensity at Eu $4d{-}4f$ absorption edge region. The $4f$ electrons of Eu atoms are excited selectively and locally, when the photon energy is tuned to the Eu $4d{-}4f$ intra-ion transition. The relaxation of the excited ions, in the photon energy region of Fano resonance, leads to the emission of additional electrons. At the resonance energy two effects may occur. The usual photoemission from Eu $4f$ orbital expressed by the formula:

$$\text{Eu } 4d^{10}4f^7 + h\nu \rightarrow \text{Eu } 4d^{10}4f^6 + \bar{\text{e}}$$

and an additional super-Coster–Kronig decay channel when electrons are emitted from Eu ions according to the following formula:

$$\text{Eu } 4d^{10}4f^7 + h\nu \rightarrow [\text{Eu } 4d^9 4f^8]^* \rightarrow \text{Eu } 4d^{10}4f^6 + \bar{\text{e}}, \qquad (^*\text{excited state}).$$

The Fano-like resonance is the result of the interference between the direct photoemission process of Eu $4f$ electrons and the discrete Eu $4d{-}4f$ transition, followed by a super-Coster–Kronig decay. The Fano asymmetric line shape [9] includes a maximum and a minimum called resonance and antiresonance, respectively. The value for the resonance energy of Eu $4d \rightarrow 4f$ transition for Eu^{2+} ions is about 141 eV and antiresonance energy — 132 eV while for Eu^{3+} ions it is about 146 and 132 eV, respectively. For resonant $h\nu$ energy, the increase of Eu $4f$ states contribution to the measured energy distribution of photoemitted electrons appears. The comparison of the spectra recorded for photon energies corresponding to the resonance and antiresonance enabled us to determine the contribution of $4f$ electrons to the valence band.

3. Experimental conditions

The $Te/Eu_{1-x}Gd_xTe$ layers were grown by MBE method on BaF_2 (111) substrate. An EuTe layer of the thickness of about 50 nm was deposited as a buffer layer on the substrate. Then the stream of Gd atoms was added to the growing EuTe layer and $Eu_{1-x}Gd_xTe$ layer with a thickness of several nm was obtained. The protective layer of Te with the thickness of several nm was deposited on top of the layer. Developing methods of preparation of clean (EuGd)Te crystals without trivalent europium species is important for practical application of this material.

The photoemission data were obtained with the Tunable VUV Photoelectron Spectrometer at the beam line E1 (FLIPPER II) of DORIS storage ring at HASYLAB (Hamburg, Germany). An excitation energy was chosen in the range between 100 and 200 eV which covers regions of $4d-4f$ Fano resonances for both Eu^{2+} and Eu^{3+} ions. The energy distribution curves (EDCs) were measured in the region of electron binding energy starting from the valence band edge down to the Te $4d$ (40 eV) core level.

4. Results and discussion

Figure 1 presents the process of the energy distribution curve formation. The structure of the occupied electronic states of the crystal manifests itself in the energy distribution of electrons emitted into vacuum due to photon absorption in the crystal.

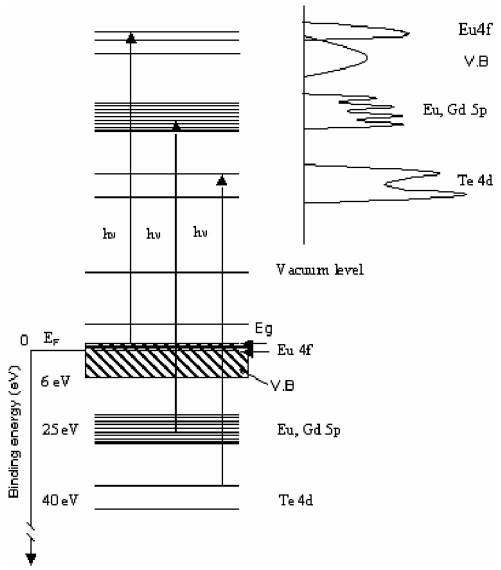

Fig. 1. The model of the energy distribution curve creation.

In the case of the Eu compounds the ions with different valence show a different behavior: the resonant energy Eu $4d \rightarrow 4f$ is different for Eu ions in divalent or trivalent chemical states and the final state multiplets $4f^5$ and $4f^6$ lie at different binding energies [10, 11]. In Te/EuGdTe layer the Eu $4f$ electrons are located at the valence band edge region for Eu $^{2+}$ ions while for Eu^{3+} ions they are located at 5–8.5 eV below it. Figure 2 shows the set of EDCs at $h\nu = 141$ eV, which corresponds to the resonance of Eu^{2+}, measured after different annealing processes for EuGdTe layer with protecting layer of tellurium. The parameters describing the shape of Fano type resonance was determined from the set of measured EDCs.

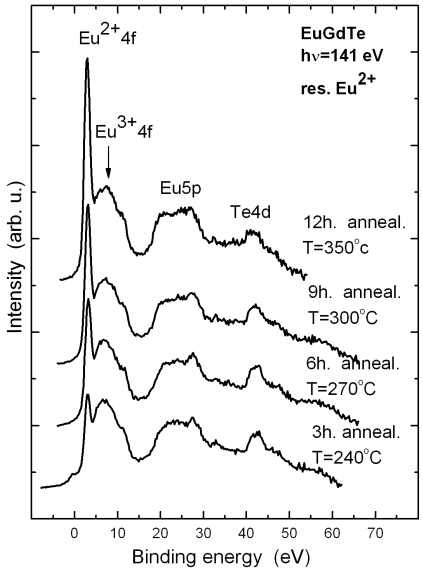

Fig. 2. The set of EDCs of Te/EuGdTe layers at resonance energy for Eu^{2+} ions ($h\nu =$ 141 eV) after annealing.

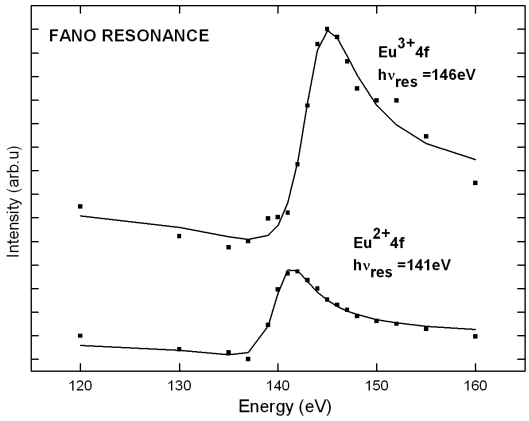

Fig. 3. Fano resonance curve (Constant Initial State curve) for Eu^{2+} and Eu^{3+} ions of Te/EuGdTe layers after annealing.

The shape of Fano resonance (presented in Fig. 3) can be expressed as:

$$I(h\nu) = I_0 \frac{(\varepsilon + q)^2}{I + \varepsilon^2},$$

where $\varepsilon = (E_R - h\nu)/(\Gamma/2)$, Γ describes spectral width of the autoionized discrete state, q is Fano's asymmetry parameter and I_0 is the intensity of nonresonant photoemission.

The annealing of the sample after sputtering leads to the change of the ratio of the heights of peaks corresponding to Eu^{2+} and Eu^{3+} ions (see Fig. 2). Sequential heating of the sample at 350°C under UHV conditions, leads to the remarkable increase of the peak corresponding to Eu^{2+} and decrease of the peak corresponding to Eu^{3+} ions. This effect corresponds to the change of the structure of defects occurring in the sample, induced by the annealing. It leads to the improvement of the electronic properties of (EuGd)Te layer.

5. Summary

The Te/EuGdTe MBE layers subjected to different annealing processes were investigated by resonant photoemission with the use of synchrotron radiation. Two Fano-type resonance energies at 141 eV and 146 eV were determined for Eu^{2+} and Eu^{3+} ions, respectively. The amount of Eu^{3+} ions in the sample strongly depends on annealing conditions and decreases with increasing annealing time and temperature.

Acknowledgments

Authors acknowledge support of grants 1 P03B 053 26, 72/E- 67/SPB/ DESY/P-03/DWM68/2004–2006 and European Commission contract RH3- -CT-2004-506008(IA=SFS) European Community program G1MA-CT-2002-4017 (Center of Excellence CEPHEUS).

References

[1] A. Mauger, C. Godart, *Phys. Rep.* **141**, 51 (1986).

[2] G.A. Prinz, *Science* **282**, 1660 (1998).

[3] I. Zutic, J. Fabian, S. Das Sarma, *Rev. Mod. Phys.* **76**, 324 (2004).

[4] S. Hüfner, *Photoelectron Spectroscopy, Springer Series in Solid-State Science*, Vol. 82, Springer, Berlin 1995.

[5] L. Ley, M. Cardona, *Photoemission in Solids I and II, Topics in Applied Physics*, Vols. 26/27, Springer, Berlin 1979.

[6] *Solid-State Photoemission and Related Methods*, Eds. W. Schattke, M.A. Van Hove, Wiley-VCH, Berlin 2003.

[7] S.L. Molodtsov, M. Richter, S. Danzenbächer, S. Wieling, L. Steinbeck, C. Laubschat, S.A. Gorovikov, *Phys. Rev. Lett.* **78**, 142 (1997).

[8] C.G. Olson, P.J. Benning, M. Schmidt, D.W. Lynch, P. Canfield, *Phys. Rev. Lett.* **76**, 4265 (1996).

[9] U. Fano, *Phys. Rev.* **124**, 1866 (1961).

[10] W.D. Scheider, C. Laubschat, G. Kalkowski, *Phys. Rev. B* **28**, 2017 (1983).

[11] N. Martensson, B. Reihl, W.D. Schneider, *Phys. Rev B* **25**, 1446 (1982).